American Journal of Pathology, Vol. 147, No. 6, December 1995

Comparison of Intracerebral Inoculation and Osmotic Blood-Brain Barrier Disruption for Delivery of Adenovirus, Herpesvirus, and Iron Oxide Particles to Normal Rat Brain

Leslie L. Muldoon,* Gajanan Nilaver,*† Robert A. Kroll,† Michael A. Pagel,†‡ Xandra O. Breakefield,§ E. Antonio Chiocca,§ Beverly L. Davidson,‖ Ralph Weissleder,¶ and Edward A. Neuwelt†‡#

From the Department of Cell and Developmental Biology, Department of Neurology,† Department of Biochemistry and Molecular Biology and Division of Neurosurgery,* Oregon Health Sciences University, and Veterans Administration Medical Center,‡ Portland, Oregon; Department of Neurology and Neuroscience Program and Massachusetts General Hospital Cancer Center,§ Harvard Medical School and Massachusetts General Hospital–East, Charlestown, Massachusetts; Department of Internal Medicine,‖ University of Iowa College of Medicine, Iowa City, Iowa; and Magnetic Resonance Pharmaceutical Program, Massachusetts General Hospital Nuclear Magnetic Resonance Center,¶ Harvard Medical School, Charlestown, Massachusetts*

Delivery of adenovirus, herpes simplex virus (HSV), and paramagnetic monocrystalline iron oxide nanoparticles (MION) to rat brain (n = 64) was assessed after intracerebral inoculation or osmotic disruption of the blood-brain barrier (BBB). After intracerebral inoculation, the area of distribution was 7.93 ± 0.43 mm² (n = 9) for MION and 9.17 ± 1.27 mm² (n = 9) for replication-defective adenovirus. The replication-compromised HSV RH105 spread to 14.00 ± 0.87 mm² (n = 8), but also had a large necrotic center (3.54 ± 0.47 mm²). No infection was detected when virus was administered intra-arterially without hyperosmotic mannitol. After osmotic BBB disruption, delivery of the viruses and MIONs was detected throughout the disrupted cerebral cortex. Positive staining was found in 4 to 845 cells/100 μm thick coronal brain section (n = 7) after adenovirus administration, and in 13 to 197 cells/section (n = 8) after HSV administration. Cells of glial morphology were more frequently stained after administration of adenovirus, whereas neuronal cells were preferentially stained after delivery of both HSV vectors and MION. In a preliminary test of vector delivery in the feline, MION was detected throughout the white matter tracts after inoculation into normal cat brain. Thus MION may be a tool for use in vivo, to monitor the delivery of virus to the central nervous system. Additionally, BBB disruption may be an effective method to globally deliver recombinant viruses to the CNS. (Am J Pathol 1995, 147:1840–1851)

We have previously characterized a feline model of human Sandhoff disease (G_{M2}-gangliosidosis, β-hexosaminidase deficiency), which results from the mutation of a single gene.[1] This model provides an excellent opportunity to study issues in central nervous system (CNS) gene therapy.[2] Gene therapy of the CNS with recombinant viral vectors is currently being studied for replacement of faulty genes in neurons or transfer of toxic genes to tumor cells.[2–4] Neurons and other postmitotic cells can be infected by both herpes simplex virus (HSV)[5–7] and adenovirus.[8,9] The HSV vectors may also be targeted to tumor cells by selective deletion of genes involved in viral replication.[10–13] However, a major impediment to both viral gene therapy of neurodegenerative diseases affecting the brain and virus-mediated treatment of brain tumors will be an adequate volume of distribution of virus delivered to the target cells in the

Supported by a Veterans Administration merit review grant to EAN, National Cancer Institute grant CA31770 to EAN, and National Institute of Neurological and Communicative Disorders and Stroke grants NS24279 to XOB and NS33618 to EAN.

Accepted for publication August 29, 1995.

Address reprint requests to Edward A. Neuwelt, M.D., Oregon Health Sciences University, L603, 3181 SW Sam Jackson Park Road, Portland, OR 97201.

CNS.[2,14] In preparation for gene therapy in the cat model, we have examined the problem of achieving wide delivery of recombinant viruses to rat brain.

A number of studies have demonstrated that viral infection can be attained in the CNS of the rat after administration of virus to brain by focal intracerebral inoculation.[3,5,8,9,13,15,16] In these studies, primary infection after focal inoculation of virus is limited to 1 to 3 mm surrounding the injection site. Inoculation with convection, which utilizes rapid flow of large volumes to enhance diffusion, may increase the volume of distribution of water-soluble compounds in brain to >1 cc,[17] although it is unclear whether convection will be a mechanism for increasing virus delivery as well. As an alternative to direct inoculation, osmotic opening of the blood-brain barrier (BBB) has been investigated as a means of delivering chemotherapeutic agents, antibodies, imaging agents, and viral particles to the brain.[2,18] The BBB is a capillary barrier that results from a single continuous layer of endothelial cells bound together with tight junctions. This layer blocks blood-borne molecules from entering the brain.[18–20] Infusion of hypertonic mannitol results in reversible shrinkage of the cerebrovascular endothelial cells and subsequent increased permeability of the tight junctions that make up the anatomical basis of the BBB.[19] We have recently demonstrated that this reversible and transient osmotic disruption of the normal BBB may be a useful mechanism to obtain more global delivery of viral particles.[13,18,21]

Delivery of viral vectors to brain by any of these routes of administration, and infection of target cells, has been demonstrated previously only after sacrifice by using immunocytochemical staining for viral proteins,[3,8] by using marker genes such as the *lacZ* gene for bacterial β-galactosidase[5,16] or therapeutic transgenes,[4,15] or by using quantitative polymerase chain reaction for viral DNA.[22] It would be useful to have a mechanism to examine the distribution of viral particles antemortem to demonstrate the tissue distribution and volume of brain subject to viral infection.

Monocrystalline iron oxide nanoparticles (MION) are superparamagnetic compounds, developed by Weissleder et al,[23,24] which can be used as contrast agents for magnetic resonance (MR) imaging. MION consist of a core iron oxide crystal 4.6 ± 1.2 nm in diameter, with a stable dextran coat yielding an overall hydrodynamic diameter of 20 ± 4 nm, unimodal size distribution. This is comparable to the diameters of adenovirus particles, (65 to 80 nm)[25] and HSV particles (120 nm).[26] We have previously shown that the distribution of these iron oxide particles can be monitored in the live animal by MR imaging and then by histochemical staining for iron after sacrifice. Furthermore, these particles can be delivered across the BBB of the rat after osmotic BBB disruption.[27] In this study, we have compared MION delivery with delivery of HSV or adenovirus after administration to rat brain by direct inoculation or osmotic BBB disruption. MION may be a useful tool to noninvasively monitor the distribution of virus after delivery to brain.

Materials and Methods

Virus Vectors

The HSV mutant RH105 lacks the HSV thymidine kinase gene (*HSV-TK*), and bears the *lacZ* gene, under control of the HSV *IE3* promoter, inserted into the *HSV-TK* locus.[28] RH105 is replication-compromised in that it can only replicate in dividing cells,[29] and it tends to downregulate immediate-early gene expression in neurons.[7] It is unable to form a lytic infection in normal brain cells (neurons and glia), which have very low levels of endogenous mammalian *TK*.[11,29] The titer of HSV RH105 was determined to be 1×10^{10} pfu/ml by a plaque-forming assay on confluent monolayers of VERO African green monkey kidney cells.[11]

The hrR3 replication-compromised HSV vector was originally obtained from Dr. S. Weller (University of Connecticut Medical School). This vector contains the *lacZ* gene in the ribonucleotide reductase gene locus, under control of the *ICP6* immediate-early viral promoter.[7,30] Like *HSV-TK*, the ribonucleotide reductase mutation allows viral replication in dividing cells, but not in nondividing cells. The hrR3 vector also has increased sensitivity to acyclovir, which will increase its antitumor efficacy. HrR3 was titered and stored as described for RH105.

The adenovirus mutant AdRSVlacZ contains a deletion in *IE1* and a partial deletion in *IE3*. The *lacZ* gene has been inserted in *IE1* under control of the Rous sarcoma virus promoter.[8,21] The loss of *IE1* renders the adenovirus vector replication-defective. Freshly purified virus in CsCl was desalted by chromatography over a G25 Sephadex column and a titer of 1.5×10^{12} particles/ml was determined by measuring absorbance at 260 nm. This concentration represents 1 to 5×10^{10} pfu/ml, as determined by plaque assay, because not all particles are infectious.[8,21]

Intracerebral Inoculation in the Rat

Animal studies were performed in accordance with guidelines established by the Oregon Health Sciences University committee on Animal Care. Adult Long-Evans rats were anesthetized with intraperitoneal (i.p.) ketamine (50 mg/kg) and xylazine (2 mg/kg). The head was shaved and the rat placed in a stereotactic frame (David Kopf Instruments, Tujunga, CA). A midline incision was made to expose the frontal bone where a 2-mm burr hole was made. The tip of a 27-gauge needle attached to a 50-μl Hamilton syringe was lowered into the right caudate putamen, using stereotactic coordinates at bregma = 0: vertical = −6.5 mm from the top of the skull; lateral = −3.1 mm. Twenty-four μl of 0.9% (w/v) saline containing adenovirus AdRSVlacZ (1×10^9 to 1×10^{11} particles, n = 10), HSV RH105 (2.4×10^8 pfu, n = 9), MION (2 to 10 μg, n = 9), hrR3 (2.4×10^8 pfu, n = 2), or the RH105 virus in combination with MION (2.4×10^8 pfu virus, 5 μg MION, n = 3) was administered over a 20-minute period. The needle was then withdrawn over a 20-minute period, and the skin closed in a single layer.

Inoculation into Feline Brain

A normal domestic cat, 4 to 5 kg, was anesthetized with i.p. sodium pentobarbital (40 mg/kg). The head was shaved and the cat placed in the stereotactic frame. The right temporalis muscle was exposed, then elevated and retracted laterally. A 4-mm burr hole was made and a 27-gauge needle attached to a 1-ml syringe was lowered into the internal capsule. The stereotactic coordinates were: ear bars = 0; lateral = 8 mm right of midline; anteroposterior = 14 mm anterior from 0, vertical = 3 mm ventral from 0. MION was inoculated at a rate of 4 μl/minutes for a total of 0.5 ml (250 μg iron). The needle was then withdrawn over a 20-minute period.

BBB Disruption

Adult Long-Evans rats, ~220 g, were anesthetized with isoflurane inhalant (5% induction, 2% maintenance) in an air atmosphere, and the carotid artery was exposed through a ventral neck incision. A catheter filled with heparinized saline was tied into the right external carotid artery for retrograde infusion. Mannitol (25% w/v in H_2O) warmed to 37°C was infused into the right internal carotid artery via the right external carotid artery catheter at a rate of 0.12 ml/s using a constant flow pump (Harvard Instruments, Newport Beach, CA) as described previously.[18,20,21] Immediately after disruption, rats received 1 ml of saline containing either adenovirus AdRSVlacZ (5×10^{11} particles, n = 7), HSV RH105 (1×10^9 pfu, n = 4), HSV hrR3 (5×10^8 pfu, n = 6) or the combination of adenovirus plus MION (10 mg/kg, n = 2), administered intra-arterially (i.a.) via the carotid catheter. Additional animals received the agents after mock disruption with i.a. saline administered in place of mannitol (n = 6 for adenovirus, 2 for adenovirus plus MION, 2 for RH105, and 2 for hrR3). Five minutes before experimental or sham BBB modification, 2% Evans blue dye was administered intravenously (2 ml/kg) to provide a qualitative marker for barrier disruption of the ipsilateral hemisphere; staining was graded as previously described.[20] Because BBB modification requires sacrifice of the internal carotid artery, the procedure can only be performed once per animal.

MR Imaging

The monocrystalline iron preparation, synthesized as described by Shen et al,[24] was imaged using a small transmit/receive coil that was built specifically for rat MR studies, as described previously.[27] Coronal T1 weighted images were obtained with a repetition time (T_R) of 300 ms, echo time (T_E) of 16 ms, 4 excitations, a 256 × 192 matrix, a 9-cm field of view, and a 3-mm slice thickness. Coronal spoiled grass images were acquired with T_R = 60 ms, T_E = 7 ms, flip angle = 45°, 9 cm field of view, in a 256 × 192 matrix, with two excitations.

Fixation and Sectioning

Animals that received adenovirus were sacrificed at day 4, and those that received HSV were sacrificed 1 to 4 days after virus administration. Rats that received MION alone were sacrificed 2 h after administration, and rats that received MION in conjunction with virus were sacrificed at 2 days (HSV) or 4 days (adenovirus) after administration. Rats were sacrificed by barbiturate overdose (i.p.), and fixed by perfusion with 10% neutral buffered paraformaldehyde. The cat that received iron was sacrificed 2 hours after inoculation by barbiturate overdose, and the brain was harvested and fixed by immersion in 10% neutral buffered formalin. Brain regions of interest were blocked in the coronal plane and postfixed in 4% (w/v) buffered paraformaldehyde for 24 h, then sectioned serially at 100 μm in the coronal plane with a Vibratome (Oxford Instruments, Bedford, MA). Tissues to be examined ultrastructurally by electron microscopy were aldehyde-fixed, postfixed in 2%

osmium tetroxide, dehydrated in ascending concentrations of ethanol, and embedded in Epon 812. Sections were cut with a diamond knife, mounted on bare copper grids, and stained with uranyl acetate and lead citrate.

Histochemistry

To stain for iron, sections were incubated in Perl's solution (equal parts of 2% HCl and 2% potassium ferrocyanide; 30 minutes at room temperature), rinsed in deionized water (30 minutes) and incubated in 0.5% diaminobenzidine (DAB) in Tris-buffered saline (pH 7.4) containing 0.15% hydrogen peroxide, as described by Koeppen et al.[27,31] This stain yields a brown reaction product. Hematoxylin and eosin (H&E) staining for pathology was performed by standard techniques. The XGal histochemical stain for β-galactosidase (β-Gal) activity was performed as previously described.[8]

Immunocytochemistry

Antibodies used in this study were purified polyclonal (rabbit) antibodies to *Escherichia coli* β-galactosidase (Cappel Laboratories, Westchester, PA), and polyclonal antibodies against HSV capsid and core proteins (Dako, Glostrup, Denmark). Immunostaining was performed by the indirect immunoperoxidase labeling technique as previously reported.[32] Tissue sections incubated with primary antibody were reacted with biotinylated protein A followed by the ABC complex (prepared from the avidin and biotinylated peroxidase reagents provided in the Vectastain ABC kit, Vector Laboratories, Burlingame, CA). Brown reaction products were formed with DAB. For double staining either for two antigens or for iron and antibody, sections were first stained for iron or the first antigen using DAB to yield brown reaction products followed by immunostaining using benzidine dihydrochloride to yield blue labeling.[32] Selected sections were counterstained with thionine, and permanently mounted under cover slips.

Image Analysis

Slides were placed on a Zeiss *Axioplan* Universal (Carl Zeiss, Oberkochen, Germany) microscope and viewed at a low magnification so that the whole brain section was visible. A Sony CCD/RGB DXC 151 camera attached to the microscope captured the images, and a Color Snap 32+ frame grabber board converted the analog signal to digital on a Macintosh 21-inch color display. The images were analyzed using Image 1.55 software tools. For virus inoculation studies, the area of distribution in each section was determined by outlining the extent of β-Gal-positive or HSV antigen-positive cells using the pencil tools and determining the enclosed area. Similar measurements were made for MION distribution in brain sections. Each area measurement was performed three times each on two to four sections surrounding the inoculation site and the mean and standard error of the mean (SEM) for each brain and each group of brains was calculated. The number of infected cells in the BBB disruption brains was determined by examining every sixth 100 μm section (7 to 12 per brain) under 100× magnification and counting all the positively staining cells. The areas of distribution and number of positive cells were compared by Student's *t*-test. The correlation between MION histological and MR volumes was determined using the cricket graph program (Cricket Software, Malvern, PA).

Results

Comparison of MION and Virus Distribution after Delivery to Rat Brain by Focal Intracerebral Inoculation

We examined the volume of distribution of gene expression from primary infection of HSV mutants RH105 and hrR3, or adenovirus mutant AdRSVlacZ, after stereotactic inoculation of each vector into rat brain, deep in the caudate putamen of the basal ganglia. Adenovirus brains were analyzed 4 days after infection by staining for bacterial β-Gal, and brains infected with HSV were analyzed from 1 to 4 days after inoculation by staining for β-Gal or viral coat protein antigens. These times have been shown to provide the best gene expression by previous investigators[5,6,8] and in our own preliminary experiments.

The general pattern of virus infection was very similar for all three viruses, with staining detected within the caudate nucleus, in or along the corpus callosum, and some spread into cortex (Figures 1A, 2A). The vertical length of stained tissue in the coronal plane in sections around the inoculation site was ~5 mm, with no difference between vectors (Table 1). In contrast, the width of staining was significantly different between adenovirus (3.07 ± 0.27 mm, n = 9) and HSV RH105 (3.93 ± 0.15 mm, n = 8), $P < 0.001$ (Table 1). Both HSV vectors, but not adenovirus, were found to spread into the cortex of inoculated animals, resulting in a larger area of distribution

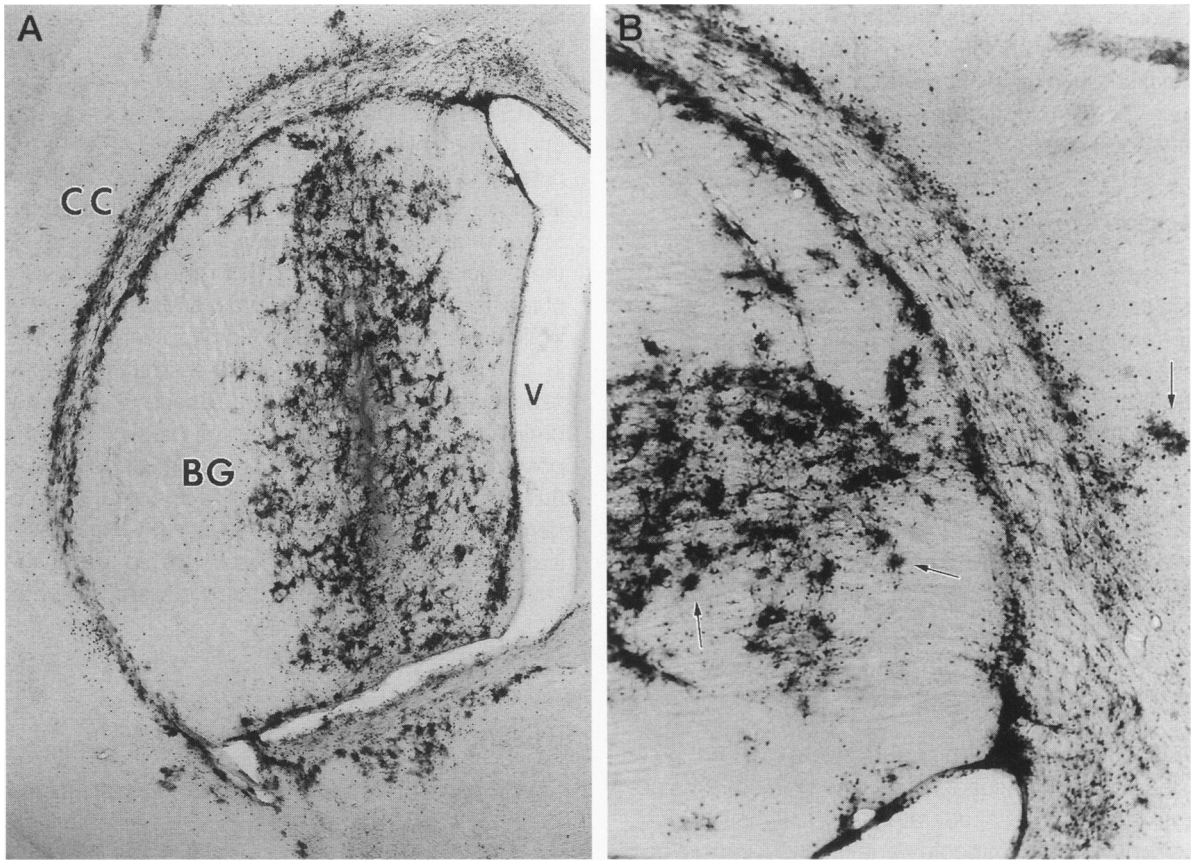

Figure 1. *Adenovirus AdRSVlacZ inoculation in rat brain.* (**A**) *Distribution of immunocytochemical staining for β-Gal in a coronal section of rat brain after focal intracerebral inoculation of adenovirus mutant AdRSVlacZ. BG, basal ganglia; CC, corpus callosum; V, ventricle* (*25×*). (**B**) *Enlarged section of the caudate nucleus and corpus callosum in* **A**, *showing primarily astrocytic infection, as indicated by the arrows and little detectable necrosis* (*50×*). **B** *has been rotated 90°. Note arrow at extreme right, showing area of gliosis which can be seen at the top of panel* **A**.

(area for RH105 = 14.54 ± 1.14 mm^2, n = 8; area for adenovirus staining = 9.17 ± 1.27 mm^2, n = 9, $P < 0.001$; Table 1). Staining in the cortex was associated with 4 days of infection with RH105 (area = 15.74 ± 0.64 mm^2, n = 5) rather than 1 or 2 days (area = 12.81 ± 0.69 mm^2, n = 6, $P < 0.01$).

After virus inoculation, parenchymal cells expressing β-Gal immunoreactivity had the morphology of both neurons and astrocytes. Adenovirus-mediated gene expression was found mostly in glial cells, with only occasional neurons being detected, whereas HSV appeared to target mostly neuronal cells (Figures 1B and 2B). The β-Gal reactivity could additionally be detected, extending along the corpus callosum, for several millimeters from the injection site. The cells labeled in this region had the morphological appearance of astrocytes after adenovirus inoculation (Figure 1B), and neurons after HSV inoculation (Figure 2B).

Infection of the brain after HSV inoculation was associated with necrosis at the inoculation site, both at the surface of the brain and within the caudate nucleus (Figure 2B), which measured 3.54 ± 0.47 mm^2 per section in the region of RH105 virus inoculation. In contrast, little evidence of neurotoxicity was seen with adenovirus inoculation, even with 1×10^{11} particles inoculated (Figure 1B). The necrotic area averaged only 0.80 ± 0.23 mm^2 per section in adenovirus brains.

We next examined MION volume of distribution after focal inoculation. Within 2 hours of inoculation of 5 μg MION, MR spoiled grass images were obtained. The MR images demonstrated iron distribution throughout the caudate nucleus, along the corpus callosum, and into the cortex of the rat (Figure 3A). Immediately after imaging, the rats were sacrificed and brain sections were stained by histochemistry for iron (Figure 3B) or by H&E for pathological examination (not shown). No evidence of necrosis could be detected on MR images or histological sections. The total volume of distribution of MION in rat brain determined from MR images was compared with image analysis of histological sections, with a correlation R^2 = 0.935. The area of distribution of

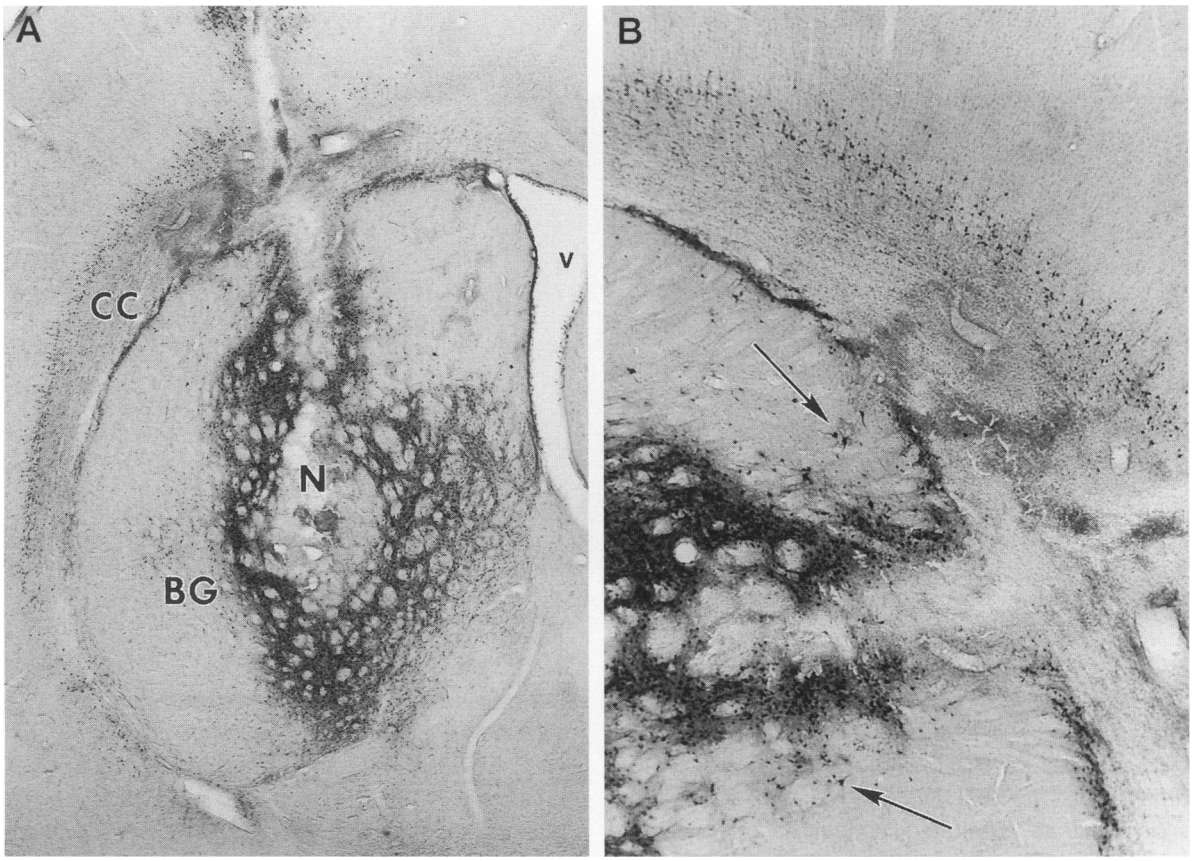

Figure 2. *HSV RH105 inoculation in rat brain.* (**A**) *Distribution of immunocytochemical staining for β-Gal in a coronal section of rat brain after focal intracerebral inoculation of HSV mutant RH105. BG, basal ganglia; CC, corpus callosum; V, ventricle; n, necrotic area* (25×). (**B**) *Enlarged section of caudate nucleus, corpus callosum, and cortex in* **A**, *showing neuronal staining at the arrows, as well as necrotic tissue at the center of the inoculation site* (50×). **B** *has been rotated by 90° as evidenced by the needle track.*

histological staining for iron in sections around the inoculation site (7.39 ± 0.43 mm^2, n = 9) was very similar to the distribution of adenovirus staining (9.17 ± 1.27 mm^2, n = 9; Table 1). When MION was administered in combination with RH105 both the area and the width of iron staining were significantly different from MION alone ($P < 0.02$). However, it is unclear whether this difference was due to the presence of virus or diffusion because of the difference in sacrifice time (2 days for MION with RH105 *versus* 2

Table 1. *Area of Distribution after Direct Inoculation into Normal Rat Brain*

Virus	Area (mm^2)	Necrotic area (mm^2)	Vertical length (mm)	Width (mm)
Adenovirus (β-Gal staining; n = 9)	9.17 (1.27)	0.80 (0.23)	5.13 (0.09)	3.07 (0.27)
RH105 (β-Gal staining; n = 8)	14.00* (0.87)	3.54* (0.47)	4.97 (0.08)	3.93* (0.15)
RH105 with MION (β-Gal staining; n = 3)	14.54 (1.14)	2.72 (0.98)	5.05 (0.16)	3.85 (0.20)
hrR3 (β-Gal staining; n = 2)	14.26 (2.43)	4.13 (0.71)	5.43 (0.12)	3.54 (0.64)
MION (iron staining; n = 9)	7.93 (0.43)	0	5.07 (0.23)	3.05 (0.14)
MION with RH105 (iron staining; n = 3)	9.43** (0.62)	2.72 (0.98)	4.88 (0.18)	3.67** (0.04)

All values are mean (SEM).

Rats received virus and/or MION stereotactically inoculated into a cerebral hemisphere, at the times and at the concentration indicated in Materials and Methods. β-galactosidase immunocytochemistry was determined for adenovirus, RH105, hrR3, and for RH105 plus MION. Iron histochemistry was performed for MION alone, and for MION plus RH105. For each brain three or four sections adjacent to the inoculation site were assessed for area of distribution of positive staining and the area of necrosis (both in mm^2), and for the vertical length and width of staining in the coronal plane. Staining in each section was determined three times, and the mean and SEM were calculated (the ranges for the hrR3 brains are shown).

*Staining for RH105 was significantly different from adenovirus or MION alone ($P < 0.001$).

**MION with RH105 iron staining was significantly greater than MION alone ($P < 0.02$).

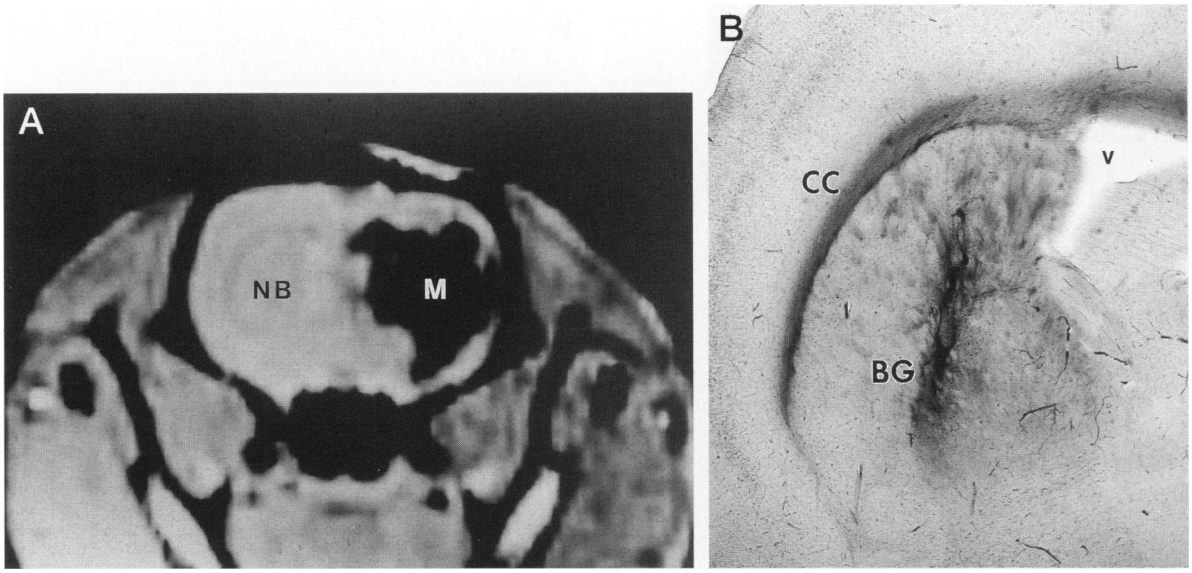

Figure 3. *MION inoculation into rat brain.* (**A**) *MR image demonstrating the distribution of the superparamagnetic label, after delivery of MION (5 μg) to rat caudate putamen. NB, normal brain; M, MION.* (**B**) *Distribution of histochemical staining for iron in a coronal section of rat brain after focal intracerebral inoculation. BG, basal ganglia; CC, corpus callosum; V, ventricle (25×).*

hours for MION alone). In contrast to adenovirus, MION staining was found predominantly in neuronal cells and fiber tracts. When MION was administered simultaneously with HSV, double labeling for iron and β-Gal demonstrated co-localization of both products in many cells that appeared to be neuronal on the basis of morphology (data not shown).

Delivery of MION and Virus to Rat Brain after Osmotic BBB Disruption

We evaluated the delivery of viruses and MION across the BBB after osmotic BBB disruption in the rat. Rats received i.a. mannitol to open the BBB followed by adenovirus or HSV, or the combination of adenovirus plus MION. Control animals received i.a. saline in place of mannitol, and virus was administered i.a. via the carotid catheter.

After administration of the adenovirus vector, the animals were sacrificed at 4 days postinfection, and the brains were sectioned and evaluated by β-Gal immunocytochemistry in every sixth 100-μm coronal section (Table 2, Figure 4). β-Gal expression was detected only in the brains of animals that received mannitol-induced disruption, and in no sections from control animals. β-Gal expression was largely confined to the disrupted right cerebral hemisphere, with some degree of crossover in the parasagittal cortex (area supplied by the anterior cerebral artery) in some sections (Figure 4A). Adenovirus-mediated β-Gal staining was observed predominantly in glial cells as assessed by morphology (Figure 4B). The positive staining of 4 to 845 cells per 100 μm coronal section was randomly distributed throughout the disrupted hemisphere, although greater cell density was detected in the cortex, hippocampus, and dentate gyrus, whereas lower levels were detected in the basal ganglia. Given the larger number of positive cells in the section shown in Figure 4 (>1 cell/mm^2), we calculate that the entire rat brain contained as

Table 2. *Delivery of Virus to Normal Rat Brains with BBB Disruption (BBBD)*

Virus/Experiment	Number	Staining	Range	Mean ± SEM	Median
Adenovirus BBBD	7	β-Gal	4–845	190 ± 106	31
RH105 BBBD	2	β-Gal	3–5		
		HSV antigens	15–22		
HSV hrR3 BBBD	6	β-Gal	1–32	6 ± 4	2
	5	HSV antigens	13–197	55 ± 32	21
Saline controls	11	β-Gal	0	0	0
	2	HSV antigens	0	0	0

Virus was delivered to normal rats by i.a. infusion with or without osmotic BBBD. Brains administered adenovirus were examined at 4 days postinfection for β-galactosidase immunocytochemistry, whereas brains that received HSVRH105 or hrR3 were stained at 2 days postinfection for both β-Gal and HSV antigens. The number of positive cells was determined in 7 to 11 100-μm sections for each stain for each brain.

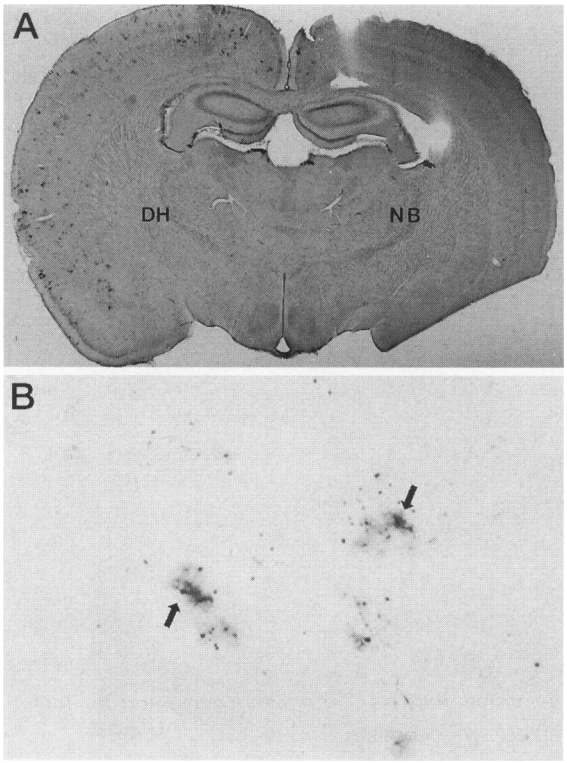

Figure 4. *Delivery of adenovirus across the BBB.* (**A**) *Distribution of immunocytochemical staining for β-Gal in a coronal section of rat brain after administration of adenovirus with BBB disruption. DH, disrupted hemisphere; NB, normal brain (16×).* (**B**) *Higher magnification of the cortex in* **A**, *showing primarily glial cell morphology, indicated by the arrows (100×).*

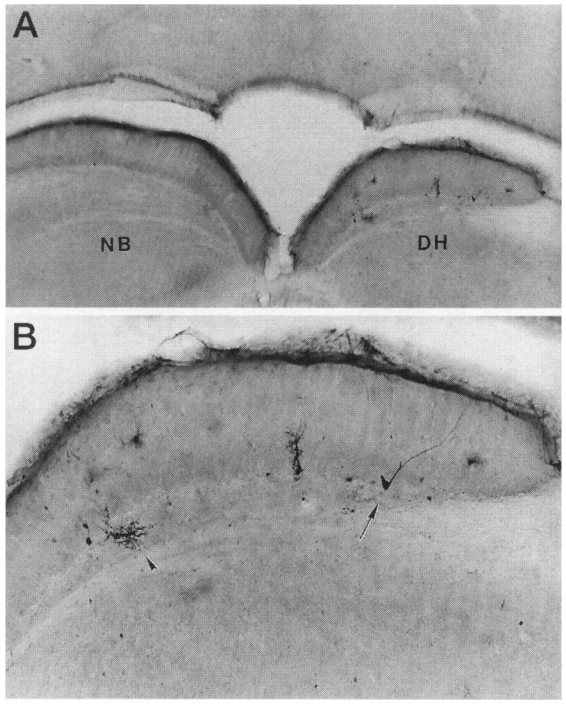

Figure 5. *Delivery of herpesvirus across the BBB.* (**A**) *Distribution of immunocytochemical staining for HSV capsid proteins in rat brain right cerebral cortex after administration of HSV RH105 with BBB disruption. DH, disrupted hemisphere; NB, normal brain (40×).* (**B**) *Higher magnification of the disrupted hemisphere in* **A**, *showing neuronal morphology* (**arrow**) *and glial cell morphology* (**arrowhead**) *(100×).*

many as 80,000 β-Gal-positive cells after delivery of adenovirus by BBB disruption.

Delivery of HSV to rat brain was evaluated at 2 days postinfection. No infection was detected in mock-disrupted animals (n = 2 for RH105, and 2 for hrR3; 8 to 10 sections examined per animal). Low levels of parenchymal cell staining for β-Gal was detected in two animals that received HSV RH105 in conjunction with mannitol to disrupt the BBB, and in six animals that received HSV hrR3. When serial sections were stained for HSV capsid antigens, a larger number of positive cells were found, 15 to 197 cells per 100-μm section (Table 2). Positive staining was sparsely but randomly distributed throughout the disrupted hemisphere, and, except for some crossover at the midline, no staining was detected in the non-disrupted hemisphere, as demonstrated in Figure 5A. Staining was found in both neural and glial cells, as assessed by morphology (Figure 5B), with some axonal processes detected as far as 1 mm from the cell body.

Positive staining for both iron and β-Gal in rat brain parenchyma was observed after simultaneous administration of adenovirus and MION with BBB disruption. Combining these two agents did not appear to reduce virus delivery to brain, as assessed by visual examination of representative sections of brains from both groups. Analysis of brain sections by electron microscopy after adenovirus and MION administration with BBB disruption demonstrated the presence of the electron-dense iron cores throughout the brain sections, and within cells morphologically identified as neurons (Figure 6).

In contrast to our previous findings of minimal toxicity with adenovirus administered after BBB disruption,[21] in the current study 4 of 11 animals that received adenovirus with mannitol, and 3 of 5 animals that received adenovirus with saline, died within 24 hours of virus administration. Nevertheless, examination of H&E-stained brain sections from surviving animals identified no signs of acute pathological abnormalities in brains that received adenovirus delivery with BBB disruption. HSV mutant RH105 was also toxic when delivered via the vasculature, with two of four rats that received RH105 with mannitol dying within 24 hours. Delivery of the hrR3 vector with BBB disruption did not result in any procedure-related deaths. However, upon sacrifice, one of the animals had widespread necrosis in the dis-

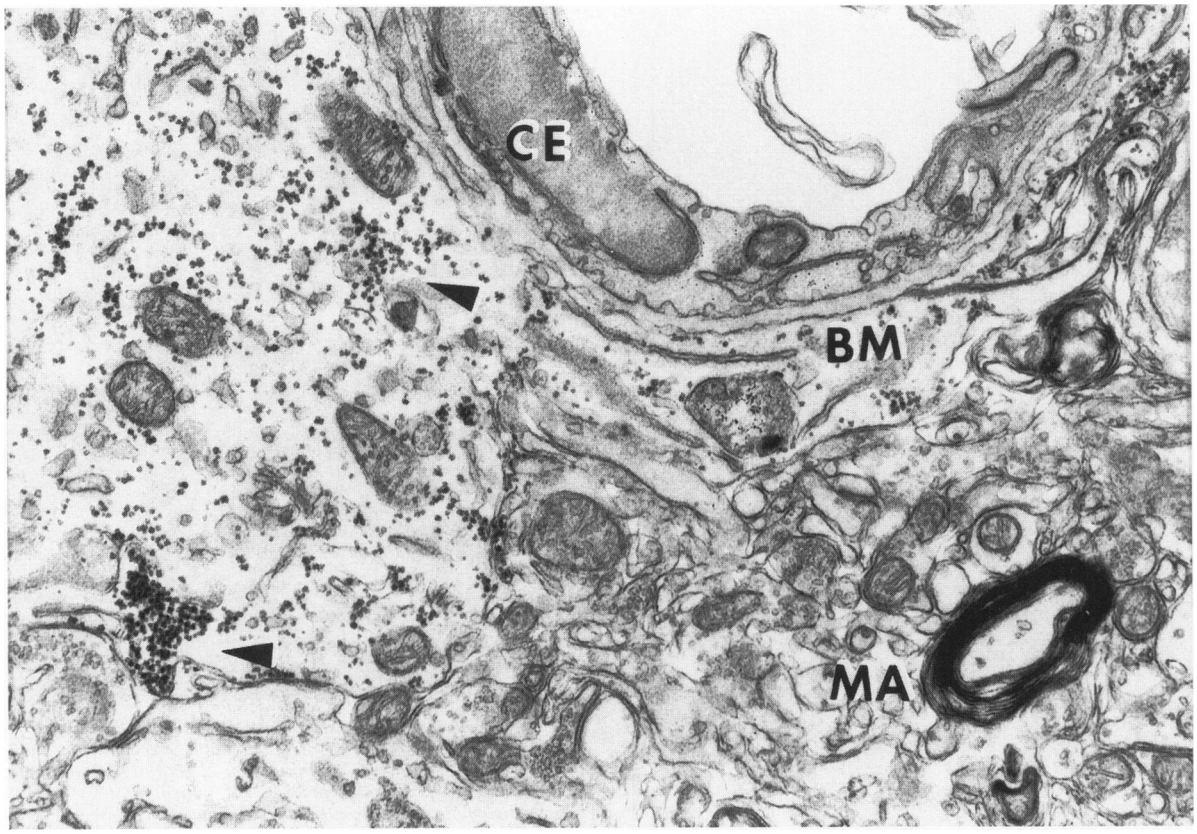

Figure 6. *Delivery of adenovirus and MION across the BBB. Electron micrograph of unstained brain tissue showing MION (electron-dense particles indicated by arrowheads) uptake in brain cells after delivery across the BBB. MA, myelinated axon; BM, basement membrane; CE, capillary endothelial cell.*

rupted hemisphere and a second had a focal area of necrosis in the disrupted cortex. No pathological abnormalities were observed in brain sections of the other surviving animals. No mock-disrupted animals (those that received i.a. virus with saline rather than mannitol) that received HSV RH105 or hrR3 died in this experiment.

Distribution of MION in Cat Brain

MION was infused into the brain of a normal feline (125 μg FeO) to test whether convection enhanced diffusion would yield widespread distribution of this virus-sized particle through an appreciable volume of feline brain. MION distribution was assessed by MR imaging and histology for iron (Figure 7). No evidence of pathological damage was observed upon examination of H&E-stained sections (data not shown).

Discussion

We have examined the delivery of recombinant viral particles and MION to rat brain through two different routes. When comparing the delivery of these particles after direct intracerebral inoculation, which is the most common method of delivery to brain, MION distribution closely resembled the distribution of cells infected by either adenovirus or the two HSV vectors, as assessed by expression of the β-Gal transgenic protein. All four agents spread a short distance through the caudate nucleus, tracked along the corpus callosum, and had some diffusion into the cortex. The significantly larger area of distribution obtained with HSV, compared with MION or adenovirus, may be due to transsynaptic transport of the replication-compromised vectors, and/or secondary infection in the cortex. Qualitatively, MION distribution also matched virus infection when these agents were administered with osmotic BBB disruption. As we have demonstrated previously for MION,[27] virus staining was found throughout the disrupted hemisphere, with some crossover at the midline. Because of these similarities, we hypothesize that MR imaging of superparamagnetic MION may be used to demonstrate the distribution of viral particles in rat brain, or in other animal models.

Figure 7. *Delivery of MION to cat brain by convection-enhanced delivery. Histochemical stain for iron after inoculation of 500 μl of solution containing MION (250 μg FeO) into the feline right internal capsule (5×).*

Use of MION provides several benefits compared with immunocytochemical or molecular analysis of virus delivery. MR imaging of this agent can be performed noninvasively, and can therefore be used to demonstrate the initial distribution of MION and viral particles in the brain in live animals.[23,24,27] MR imaging can demonstrate the entire volume of distribution of MION and virus throughout the brain tissue. This property could be used to delimit the regions where the recombinant virus may be active. In addition, when used with viral therapy of brain tumors, MR imaging with MION may demonstrate regions of the tumor that have received suboptimal amounts of virus. Finally, the histochemical stain for iron in brain sections *in vitro* provides a simple and powerful method for identifying the tissues that received particles,[27,31] which can then be tested for biochemical changes associated with therapeutic viral transgenes.

A possible drawback to the use of MION to demonstrate virus delivery is the potential neurotoxic effect of iron infused into the brain, particularly in nigrostriatal dopaminergic neurons.[33,34] The iron in the MION used in this study is protected from the extracellular environment by the dextran coat, and is a single crystal, rather than the ferrous or ferric ions in solution that are used for iron toxicity studies.[33,34] Although MION may be degraded in neuronal lysosomes and released as free iron, we have observed no signs of chronic toxicity (neither systemic toxicity nor neuropathology) of these procedures in rats studied for periods up to 3 months (RA Kroll, manuscript in preparation). In addition, in terms of imaging virus infection, the strong iron MR signal may mask potential virus toxicity, such as necrosis from replication-competent HSV.

Differential cell type infectivity of the two virus types was found in rat brain. After focal intracerebral inoculation, staining for HSV, like MION, was preferentially localized in neurons, whereas adenovirus was found in some neuronal cells but was predominantly found in cells of glial morphology. Similarly, after delivery of virus with BBB disruption, adenovirus-mediated β-Gal expression was found almost entirely in glial cells, as we have previously described.[21] In contrast, after HSV delivery both neurons and glia were positive for HSV coat protein immunocytochemistry. The molecular basis for this difference is not known. Herpesvirus has a wide host range, and can infect a variety of cell types in culture. *In vivo*, wild-type HSV is capable of infecting postmitotic neurons in the periphery and the CNS[5,6,16] and can also be passed to additional neurons in the CNS by transsynaptic transport.[5,9] It is unclear how efficiently HSV will infect glial cells *in vivo*, although infection *in vitro* has been established (our unpublished results). Less is known regarding the mechanisms of infection and uptake of adenovirus in the CNS, and it is only recently that transgene expression mediated by adenovirus vectors has been shown to occur in CNS parenchymal cells.[3,8,9] This differential targeting to neurons or glia has important implications for gene therapy. In particular, therapy of neuronal diseases with adenovirus vectors may have to rely on enzyme transfer from infected glia to affected neurons. The different cellular associations of MION and virus at the microscopic level is likely not relevant to the use of MION as a macroscopic imaging agent for MR.

A high level of toxicity was found for the viral vectors, particularly HSV, after administration by either direct inoculation or BBB disruption. At the high titers used, there may be some degree of replication and lysis in neurons caused by either incomplete latency or reversion of a small percentage of virus to wild type. Alternatively, neurotoxicity may be attributable to viral proteins in the inoculum or to an immune-mediated response. The necrosis that we found after stereotactic inoculation of virus is similar

to previous reports of long-term toxicity with the RH105 vector.[3,5,6,11] The issue of viral toxicity is being addressed by us as well as a number of other investigators. Although viral vectors are not yet optimized, both the hrR3 HSV vector and the adenovirus vector have reduced toxicity[3,8,11] and hold promise as gene delivery vehicles.[2,7]

Morbidity and mortality was observed when virus was delivered by i. a. infusion, with or without osmotic BBB disruption. The fact that mortality occurred in sham-disrupted animals that received adenovirus and had no evidence of viral gene expression in the brain suggests it may be due to systemic toxicity as a result of viral infection of nonneural tissues.[13] Our extensive animal tests have demonstrated BBB disruption to be a safe procedure.[13,18,20,21] Clinical trials of enhanced chemotherapy delivery have demonstrated the efficacy and safety of osmotic BBB disruption in human brain tumor patients.[35]

These results represent the first report of delivery of recombinant HSV-derived vectors to the brain after BBB modification. This confirms our early results showing a fourfold increase in radioactivity in the disrupted hemisphere after delivery of radiolabeled inactivated HSV across the BBB[18] and our more recent results showing delivery of live virions to normal rat brain[21] and rat brain tumor.[13] HSV delivery resulted in fewer positive CNS parenchymal cells than adenovirus, whereas for both viruses positive cells were less abundant than was seen with the delivery of MION.[27] There are several possible reasons for this phenomenon. First, these three agents may demonstrate the size limitation for delivery across the BBB: MION = 20 nm,[23] adenovirus = 70 nm,[25] HSV = 120 nm.[26] Second, the toxicity of both the HSV RH105 mutant virus and the adenovirus AdRSVlacZ, when delivered to the vasculature with or without osmotic BBB disruption, forced us to use a relatively low concentration of virus, with less HSV than adenovirus being delivered. Higher concentrations of less toxic viruses may yield comparable delivery of the two viruses, and perhaps staining comparable to the MION delivery experiments. Third, even though we have demonstrated that the BBB is open to virus, there still may be a lack of access of virus to cells distant from the capillaries. Immunocytochemical analysis of adenovirus infection after BBB disruption suggested that glial cells that were close to capillaries are most likely to be infected by this procedure.[21] Our inoculation experiments demonstrated that HSV appeared to target neurons rather than glia. Perhaps the selectivity that the HSV vector demonstrated for neurons, combined with relative abundance of astrocyte foot processes at the disrupted BBB, may decrease HSV infectivity in comparison to adenovirus. This property of low infection of normal brain with HSV delivered by osmotic BBB disruption may actually be an advantage in future tests of gene therapy of tumors. Nevertheless, our results demonstrate that CNS parenchymal cells, including neurons, were stained after delivery of HSV after BBB disruption, indicating that BBB disruption may be an effective method for global delivery of virus for CNS gene therapy.

References

1. Muldoon LL, Pagel MA, Neuwelt EA, Weiss DL: Characterization of the molecular defect in a feline model for type II G_{M2}-gangliosidosis (Sandhoff disease). Am J Pathol 1994, 144:1109–1118
2. Neuwelt EA, Pagel MA, Geller AI, Muldoon LL: Gene replacement therapy in the central nervous system: viral vector mediated therapy of global neurodegenerative disease. Behav Brain Sci 1995, 18:1–9
3. Boviatsis, EJ, Chase M, Wei MX, Tamiya T, Hurford RK Jr, Kowall NW, Tepper RI, Breakefield XO, Chiocca EA: Gene transfer into experimental brain tumors mediated by adenovirus, herpes simplex virus, and retrovirus vectors. Hum Gene Ther 1994, 5:183–191
4. Davidson BL, Doran SE, Shewach DS, Latta JM, Hartman JW, Roessler BJ: Expression of *Escherichia coli* β-galactosidase and rat HPRT in the CNS of *Macaca mulatta* following adenoviral mediated gene transfer. Exp Neurol 1994, 125:258–267
5. Huang Q, Vonsattel J-P, Schaffer PA, Martuza RL, Breakefield XO, DiFiglia M: Introduction of a foreign gene (*Escherichia coli lacZ*) into rat neostriatal neurons using herpes simplex virus mutants: a light and electron microscopic study. Exp Neurobiol 1992, 115:303–316
6. Chiocca EA, Choi BB, Cai W, DeLuca NA, Schaffer PA, DiFiglia M, Breakefield XO, Martuza FL: Transfer and expression of the *lacZ* gene in rat brain neurons mediated by herpes simplex virus mutants. New Biol 1990, 2:739–746
7. Smith F, Jacob D, Breakefield XO: Virus vectors for gene delivery to the nervous system. Restorat Neurol Neurosci 1995 (in press)
8. Davidson BL, Allen ED, Kozarsky KF, Wilson JM, Roessler BJ: A model system for *in vivo* gene transfer into the central nervous system using an adenoviral vector. Nature Genet 1993, 3:219–223
9. Le Gal La Salle G, Robert JJ, Berrard S, Ridoux V, Stratford-Perricaudet LD, Perricaudet M, Mallet J: An adenovirus vector for gene transfer into neurons and glia in the brain. Science 1993, 259:988–990
10. Martuza RL, Malick A, Markert JM, Ruffner KL, Coen DM: Experimental therapy of human glioma by means

of a genetically engineered virus mutant. Science 1991, 252:854–856
11. Boviatsis EJ, Park JS, Sena-Esteves M, Kramm CM, Chase M, Efird JT, Wei MX, Breakefield XO, Chiocca EA: Long-term survival of rats harboring brain neoplasms treated with ganciclovir and a herpes simplex virus vector that retains an intact thymidine kinase gene. Cancer Res 1994, 54:5745–5741
12. Chen S-H, Shine HD, Goodman JC, Grossman RG, Woo SLC: Gene therapy for brain tumors: regression of experimental gliomas by adenovirus-mediated gene transfer *in vivo*. Proc Natl Acad Sci USA 1994, 91:3054–3057
13. Nilaver G, Muldoon LL, Kroll RA, Pagel MA, Breakefield XO Davidson BL, Neuwelt EA: Delivery of herpes virus and adenovirus to nude rat intracerebral tumors following osmotic blood-brain barrier disruption. Proc Natl Acad Sci USA 1995, 21:9829–9833
14. Ram Z, Culver KW, Oshiro EM, Viola JJ, DeVroom HL, Otto E, Long Z, Chiang Y, McGarrity GJ, Muul LM, Katz D, Blaese RM, Oldfield EH: Summary of results and conclusions of the gene therapy of malignant brain tumors clinical study. Presented at American Association of Neurological Surgeons Meeting, Orlando, FL April 22–27, 1995
15. Wolfe JH, Deshmane SL, Fraser NW: Herpesvirus vector gene transfer and expression of β-glucuronidase in the central nervous system of MPS VII mice. Nature Genet 1982, 1:379–384
16. Fink DJ, Sternberg LR, Weber PC, Mata M, Goins WF, Glorioso JC: *In vivo* expression of β-galactosidase in hippocampal neurons by HSV-mediated gene transfer. Hum Gene Ther 1992, 3:11–19
17. Bobo RH, Laske DW, Akbasak A, Morrison PF, Dedrick RL, Oldfield EH: Convection-enhanced delivery of macromolecules in the brain. Proc Natl Acad Sci USA 1994, 91:2076–2080
18. Neuwelt EA, Pagel MA, Dix RD: Delivery of UV-inactivated [^{35}S]-herpesvirus across the BBB after osmotic modification. J Neurosurg 1991, 74:475–479
19. Rapoport SI, Robinson PJ: Tight-junctional modification as the basis of osmotic opening of the blood-brain barrier. Ann NY Acad Sci 1986, 481:250–2567
20. Neuwelt EA: Blood-brain barrier disruption in the treatment of brain tumors: animal studies. Implications of the Blood-Brain Barrier and Its Manipulation, vol 2, Clinical Implications. Edited by EA Neuwelt. New York, Plenum Press, New York, 1989, pp 107–194
21. Doran SE, Ren XD, Betz AL, Pagel MA, Neuwelt EA, Roessler BJ, Davidson BL: Gene Expression from recombinant viral vectors in the CNS following blood-brain barrier disruption. Neurosurgery, 1995, 36:965–970
22. Ramakrishnan R, Fink DJ, Jiang G, Desai P, Glorioso JC, Levine M: Competitive quantitative PCR analysis of herpes simplex virus type 1 DNA and latency associated transcript RNA in latently infected cells of the rat brain. J Virol 1994, 68:1864–1873
23. Weissleder R Elizondo G, Wittenberg J, Lee AS, Josephson L, Brady TJ: Ultrasmall superparamagnetic iron oxide: an intravenous contrast agent for assessing lymph nodes with MR imaging. Radiology 1990, 175: 494–498
24. Shen T, Weissleder R, Papisov M, Bogdanov A Jr, Brady TJ: Monocrystalline iron oxide nanocompounds (MION): physicochemical properties. Magn Reson Med 1993, 29:599–604
25. Horne RW, Bonner S, Waterson AP, Wildly P: The icosahedral form of an adenovirus. J Mol Biol 1959, 1:84–86
26. Roizman B, Batterson W: Herpesviruses and their replication. Virology. Edited by BN Fields. New York, Raven Press, 1985, pp 497–526
27. Neuwelt EA, Weissleder R, Nilaver G, Kroll RA, Roman-Goldstein S, Szumowski J, Pagel MA, Jones RA, Remsen LG, McCormick CI, Shannon EM, Muldoon LL: Delivery of virus sized iron oxide particles in rodent CNS neurons. Neurosurgery 1994, 34:777–784
28. Ho DY, Mocarski ES: β-galactosidase as a marker in the peripheral and neural tissues of the herpes simplex virus vectors. Virol 1988, 167:279–283
29. Coen DM, Goldstein DJ, Weller SK: Herpes simplex virus ribonucleotide reductase mutants are hypersensitive to acyclovir. Antimicrob Agents Chemother 1989, 1395–1399
30. Coen DM, Kosz-Vnenchak M, Jacobson JG, Leib DA, Bogard CL, Schaffer PA, Tyler KL, Knipe DM: Thymidine kinase-negative herpes simplex virus mutants establish latency in mouse trigeminal ganglia but do not reactivate. Proc Natl Acad Sci USA 1989, 86:4736–4740
31. Koeppen AH, Borke RC: Experimental superficial siderosis of the central nervous system. I. Morphological observations. J Neuropathol Exp Neurol 1991, 50:579–549
32. Nilaver G, Kozlowski GP: Comparison of the PAP and ABC immunocytochemical techniques. Techniques in Immunocytochemistry, vol 4. Edited by GR Bullock, P Petrusz. London, Academic Press, 1989, pp 199–216
33. Sengstock GJ, Olanow CW, Menzies RA, Dunn AJ, Arendash GW: Infusion of iron into the rat substantia nigra: nigral pathology and dose-dependent loss of striatal dopaminergic markers. J Neurosci Res 1993, 35:67–82
34. Zhang Y, Tatsuno T, Carney JM, Mattson MP: Basic FGF, NFG, and IGFs protect hippocampal and cortical neurons against iron-induced degeneration: J Cereb Blood Flow Metabol 1993, 13:378–388
35. Neuwelt EA, Goldman D, Dahlborg SA, Crossen J, Ramsey F, Goldstein SM, Braziel R, Dana B: Primary CNS lymphoma treated with osmotic blood-brain barrier disruption: prolonged survival and preservation of cognitive function. J Clin Oncol 1991, 9:1580–1590